Journal of Materials Chemistry C

Accepted Manuscript

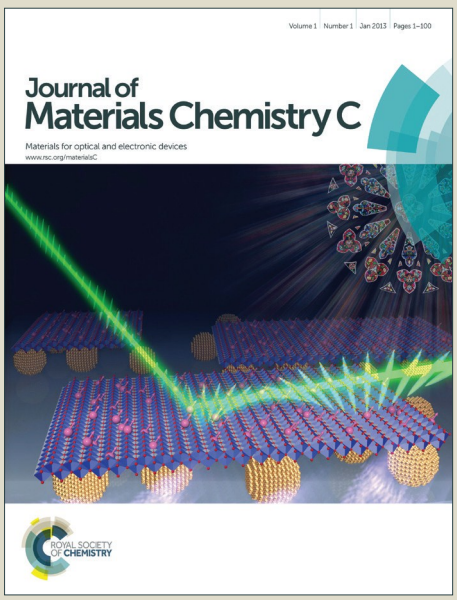

ROYAL SOCIETY OF CHEMISTRY

www.rsc.org/materialsC

Journal of Materials Chemistry C

RSCPublishing

ARTICLE

(3Z,3'Z)-3,3'-(Hydrazine-1,2-diylidene)bis(indolin-2-one) as a new electron-acceptor building block for donor-acceptor π-conjugated polymers for organic thin film transistors

Cite this: DOI: 10.1039/x0xx00000x

Received 00th January 2012,
Accepted 00th January 2012

DOI: 10.1039/x0xx00000x

www.rsc.org/

Wei Hong,[a] Chang Guo,[a‡] Bin Sun,[a‡] and Yuning Li*[a]

(3Z,3'Z)-3,3'-(Hydrazine-1,2-diylidene)bis(indolin-2-one) (HBI) containing an azine linkage is used as a novel amide-based π-conjugated electron-accepting building block for constructing donor-acceptor (D-A) π-polymer semiconductors. Copolymers of HBI and bithiophene are synthesized, which show small optical band gaps (~1.6 eV) and quite low-lying highest occupied molecular orbital (HOMO) and lowest unoccupied molecular orbital (LUMO) energy levels (E_{HOMO} = -5.6 eV; E_{LUMO} = -4.0 eV). The spin-coated polymer thin film are highly crystalline with favoured edge-on lamellar chain packing motif, which exhibit high ambipolar charge transport performance with hole and electron mobilities up to 0.11 and 0.035$cm^2V^{-1}s^{-1}$, respectively.

Introduction

Polymer semiconductors are very promising materials to enable printed electronics that can be manufactured at low cost and used for a wide range of applications such as radio frequency identification (RFID) tags, flexible displays, solar cells, memory devices, and sensors.[1-5] Among them, an emerging class of polymer semiconductors based on the combination of electron donor (D) and acceptor (A) units have demonstrated superior performances in organic photovoltaic (OPV)[6-11] and organic thin film transistor (OTFT) devices.[10-12] The favourable strong interchain interaction enabled by the static attraction of D and A units in these D-A polymers could shorten the π-π-stacking distance to reduce the energy barrier for charge hopping. High hole mobilities exceeding 10 $cm^2V^{-1}s^{-1}$ [13-15] and electron mobilities over 6 $cm^2V^{-1}s^{-1}$ [16, 17] have been recently achieved by D-A type conjugated polymers. New building blocks, especially electron acceptors, have contributed greatly to the achievement of the high charge carrier mobility and have been continuously explored to further boost the OTFT performance.[11]

One particular type of electron acceptors, amide/imide structures[18] such as naphthalene-bis(dicarboximide) (NDI), diketopyrrolopyrrole (DPP), and isoindigo (IID), have shown remarkable charge transport performance.[10-12, 19] Recently we reported a new amide-based conjugated structure, 3,3'-(ethane-1,2-diylidene)bis(indolin-2-one) (EBI, Scheme 1), which was used as an electron acceptor to form D-A polymers.[20] The EBI-based polymers such as **PEBIBT-24** (Scheme 1) were found to have short π-π stacking distances (~3.5 nm) and showed promising p-channel OTFT performance with hole mobility as high as 0.044 $cm^2V^{-1}s^{-1}$.

In this study we replaced the ethane-1,2-diylidene linkage in EBI with hydrazine-1,2-diylidene through a simple chemistry to result in a new building block, (3Z,3'Z)-3,3'-(hydrazine-1,2-diylidene)bis(indolin-2-one) (HBI, Scheme 1). The azine linkage (C=N–N=C) comprising hydrazine-1,2-diylidene moiety has been used for π-conjugated polymer.[21-27] However few azine-based polymers have been investigated as semiconductors.[28] Therefore a study on the azine-containing HBI compounds may not only provide a novel building block for conjugated polymers, but also give a better understanding of

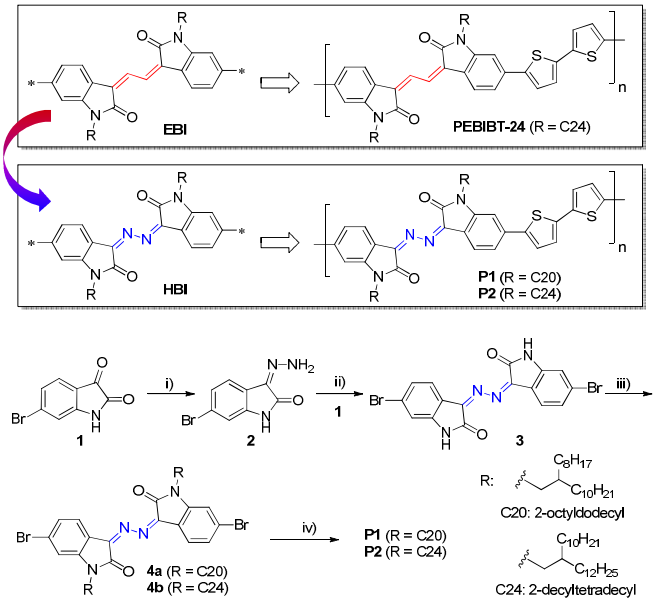

Scheme 1 Structures of EBI and HBI and the synthetic route to HBI-based polymers **P1** and **P2**: i) hydrazine hydrate/ ethanol, 50 °C, 16 h, 68.4%; ii) AcOH (catalyst)/EtOH, reflux, 4 h, 94.6%; iii) K_2CO_3, DMF, 50 °C, 60 h, 41.9% (**4a**) and 36.1% (**4b**); iv) $Pd_2(dba)_3$/P(o-tolyl)$_3$, chlorobenzene, 90 °C, 72 h, 97.1% (**P1**) and 44.6% (**P2**).

the semiconducting properties of the azine-containing polymers. Previously, a DPP-azine polymer was found to be a high performance ambipolar semiconductor showing balanced hole and electron mobilities of ~0.4 $cm^2V^{-1}s^{-1}$, indicating that azine is a strong electron-withdrawing moiety.[28] It is thus expected that the HBI block would be a stronger electron acceptor than EBI. We found that polymers based on this new building block indeed possess lower energy levels and exhibited pronounced electron transport characteristics. Ambipolar charge transport with high charge carrier mobilities were observed for the OTFT devices using these new HBI-based polymers.

Results and discussion

The dibrominated HBI compound **3** without *N*-substitution was conveniently prepared by reacting 6-bromoisatin with (Z)-6-bromo-3-hydrazonoindolin-2-one (Scheme 1) using a modified procedure for the synthesis of other HBI derivatives.[29, 30] Alkylation of **3** with 2-octyldecyl iodide and 2-decyltetradecyl iodide afforded the HBI monomers **4a** and **4b**. Stille coupling polymerization of **4a** and **4b** with 5,5'-bis(trimethylstannyl)bithiophene using $Pd_2(dba)_3$/P(o-tolyl)$_3$ as a catalyst produced the target polymers **P1** and **P2**, respectively. The polymers were purified with Sohxlet extraction with acetone and hexane to remove oligomers and catalyst residues, and finally dissolved with chloroform. Yields of **P1** and **P2** from the chloroform extractions are 97 and 45%, respectively. The lower yield of **P2** is due to the good solubility of its low molecular weight fractions in hexane (54%). **P1** and **P2** showed significantly improved solubility in comparison with the EBI-based polymers. The number average molecular weight (M_n)/polydispersity (PDI) are 40.0 kD/2.23 for **P1** and 49.8 kD/1.76 for **P2** determined by gel-permeation chromatography (GPC) at 50 °C using chlorobenzene as an eluent with polystyrene as standards. On the other hand, a high-temperature GPC at 140 °C was required to determine the molecular weight of the EBI-based polymers due to their strong aggregation in solution at lower temperatures.[20]

P1 and **P2** in chloroform showed the wavelength of maximum absorbance (λ_{max}) of 707 and 705 nm, respectively (Fig. 1). The slightly lower λ_{max} of **P2** might be caused by stronger interaction of its larger C24 side chains with the solvent molecules to make the backbone slightly more twisted than **P1** bearing C20 side chains. Similar phenomenon was observed for other polymers.[31] As-coated **P1** and **P2** films exhibited slightly blue shift λ_{max} at 702 and 701 nm,

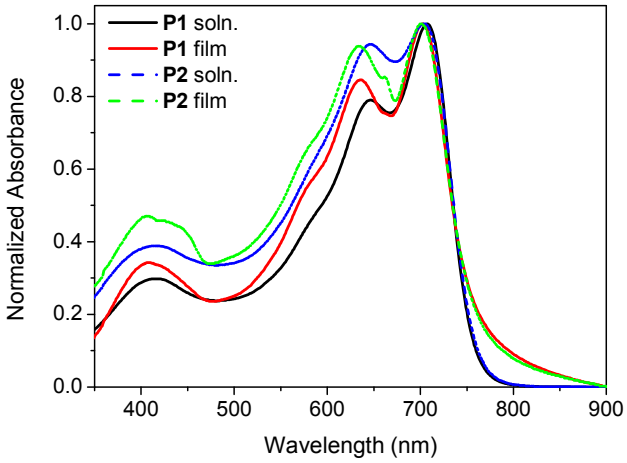

Fig.1 Normalized UV-Vis absorption spectra of **P1** and **P2** solutions in chloroform and thin films spin-coated on glass substrates (non-annealed).

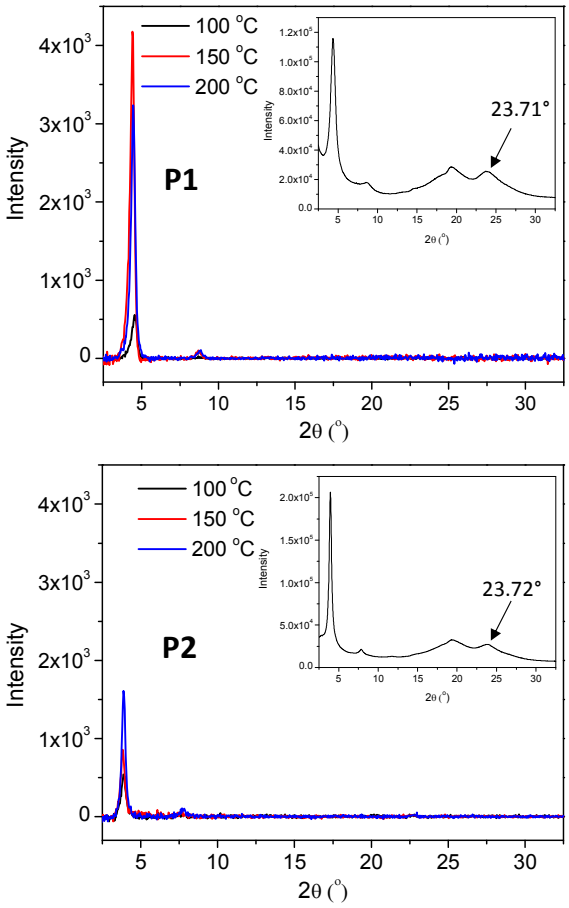

Fig.2 Reflection XRD diagrams of **P1** and **P2** thin films (~35 nm) spin-coated on dodecyltrichlorosilane-modified SiO_2/Si substrates and annealed at different temperatures with Cu Kα radiation (λ = 1.5406 Å). Inserts are the transmission XRD diagrams of polymer flakes (non-annealed) sandwiched between two Mylar substrates.

respectively. All polymer films annealed at 100, 150, and 200 °C retained almost the same λ_{max} at 701 nm (ESI†) despite of their improved chain ordering (see the XRD discussion later). The blue shift in λ_{max} from solution to the solid state observed for these two polymers is probably due to the formation of H-aggregates, where the same type of chromophores are aligned in a side-by-side manner,[32-35] resulting in a larger band gap to outweigh the band gap narrowing effect caused by the backbone planarization. This indicates that the polymer chains may be prone to packing in the D···D / A···A fashion rather than the D···A fashion, resulting in a weaker interchain interaction than in the J-aggregates. This might explain the much improved solubility of **P2** compared with its exact EBI analogue, **PEBIBT-24**. The optical band gaps of **P1** and **P2** were estimated from their onset absorption wavelengths to be E_g^{opt} = ~1.6 eV, which are similar to that of **PEBIBT-24**.[20]

The highest occupied molecular orbital (HOMO) and lowest unoccupied molecular orbital (LUMO) energy levels of **P1** and **P2** were determined by cyclic voltammetry (CV) using ferrocene as a standard (ESI†). Both polymers showed reversible oxidation and reduction peaks, but the oxidation peaks are much stronger, suggesting that these two polymers may favour hole transport over electron transport. In comparison, **PEBIBT-24** exhibited no reduction peak,[14] indicating that the electron withdrawing effect of the azine unit in HBI is responsible for the stable reduction peaks

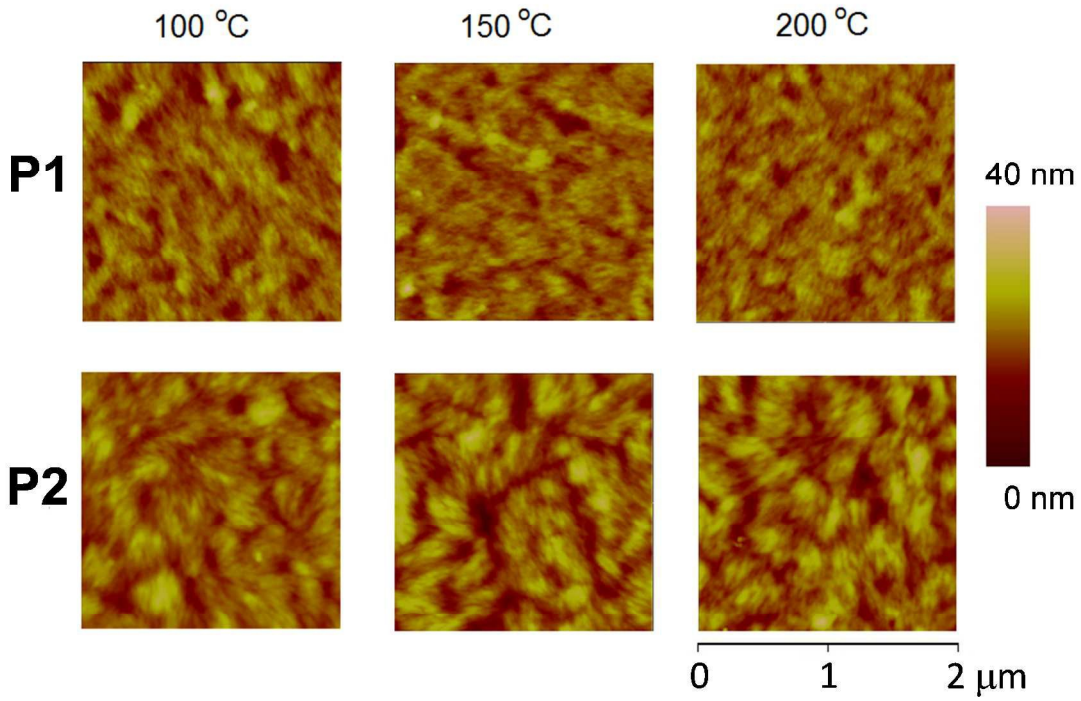

Fig. 3 Atomic force microscopy (AFM) height images of **P1** and **P2** thin films (~35 nm) spin-coated on the dodecyltrichlorosilane-modified SiO_2/Si substrates annealed at 100, 150, or 200 °C for 15 min in nitrogen.

Table 1. Summary of performance of OTFT devices using **P1** and **P2** as channel semiconductors.

Polymer	Anneal. Temp.[a] (°C)	n-type				p-type			
		Average Mobility[b] ($cm^2V^{-1}s^{-1}$)	Standard Deviation	Best Mobility[b] ($cm^2V^{-1}s^{-1}$)	V_{th} (V)[c]	Average Mobility[d] ($cm^2V^{-1}s^{-1}$)	Standard Deviation	Best Mobility[d] ($cm^2V^{-1}s^{-1}$)	V_{th} (V)[c]
P1	100	6.3×10^{-3}	1.7×10^{-3}	8.6×10^{-3}	47.4~55.2	4.1×10^{-2}	1.8×10^{-2}	5.6×10^{-2}	-40.9~-57.7
	150	9.0×10^{-3}	1.7×10^{-3}	1.1×10^{-2}	49.1~52.6	5.6×10^{-2}	3.5×10^{-2}	1.0×10^{-1}	-40.8~-63.1
	200	6.6×10^{-3}	1.9×10^{-3}	8.6×10^{-3}	51.7~59.0	5.8×10^{-2}	3.1×10^{-2}	1.0×10^{-1}	-53.2~-62.6
P2	100	1.1×10^{-2}	2.6×10^{-3}	1.6×10^{-2}	53.4~57.0	5.8×10^{-2}	7.6×10^{-3}	6.8×10^{-2}	-21.8~-25.7
	150	1.2×10^{-2}	2.8×10^{-3}	1.7×10^{-2}	50.2~55.8	7.4×10^{-2}	7.5×10^{-3}	8.6×10^{-2}	-30.5~-35.8
	200	1.6×10^{-2}	4.4×10^{-3}	2.3×10^{-2}	48.8~55.1	8.0×10^{-2}	1.5×10^{-2}	1.1×10^{-1}	-36.4~-39.7
	250	2.7×10^{-2}	5.3×10^{-3}	3.5×10^{-2}	44.2~49.5	6.0×10^{-2}	1.5×10^{-2}	8.5×10^{-2}	-45.4~-51.3
	300	2.6×10^{-2}	3.5×10^{-3}	3.1×10^{-2}	44.4~52.8	5.1×10^{-2}	6.3×10^{-3}	5.9×10^{-2}	-49.5~-53.5

a) Annealing temperature. b) V_{DS} = 100 V. c) Threshold voltage. d) V_{DS} = -100 V.

observed for **P1** and **P2**. **P1** and **P2** have the same HOMO and LUMO levels of -5.6 eV and -3.7 eV, respectively, calculated from their oxidative and reductive onset potentials.[36, 37] Their HOMO levels are lower than those of their EBI analogues (-5.4 eV)[20] indicating the stronger electron withdrawing ability of HBI than that of EBI. The LUMO levels of **P1** and **P2** calculated by using the optical band gaps (E_g^{opt} = ~1.6 eV) and the HOMO levels are about -4.0 eV, which are also lower than that of **PEBIBT-24** (-3.8 eV).[20] The discrepancy of the LUMO levels determined by the CV and the optical band gap is probably due to the exciton binding energy of **P1** and **P2**.[38, 39]

Polymer thin films spin coated on SiO_2/Si wafer and annealed at 100, 150, and 200 °C were characterized using X-ray diffractometry (XRD, Fig. 2). Both **P1** and **P2** showed distinct diffraction peaks, indicating their better crystallinity than that of the EBI-based polymers that are essentially amorphous.[20] The **P1** film annealed at 100 °C showed a primary (001) diffraction peak at 2θ = 4.55°, which corresponds to a d-spacing distance of 1.94 nm. When the annealing temperature was increased to 150 °C, a much stronger primary peak along with a secondary diffraction peak was observed. Further increasing the annealing temperature to 200 °C caused a slight decrease in the intensity of the diffraction peaks. The 100 °C-annealed **P2** film showed the primary diffraction peak at 2θ = 3.88°, representing a d-spacing of 2.28 nm. The larger interlayer distance is due to the longer side chain of **P2**. Increasing the annealing temperature to 150 °C and then 200 °C improved the crystallinity of **P2** films. **P2** with C24 side chains seems less crystalline than **P1** that has a shorter C20 side chain. Since no peak representing the π-π distance (2θ = ~20-25°) was observed, two polymers likely adopted a lamellar packing motif with an edge-on orientation, which is favoured for charge transport in OTFTs.[40, 41] To reveal the π-π stacking distance, transmission XRD measurement was conducted on polymer flakes. As shown in the inserts of Fig. 2, (010) peaks at 2θ = 23.71° and 23.72° for **P1** and **P2**, respectively, are observed, which correspond to a π-π stacking distance of ~0.375 nm. This π-π distance is similar to many other π-conjugated polymers, but larger

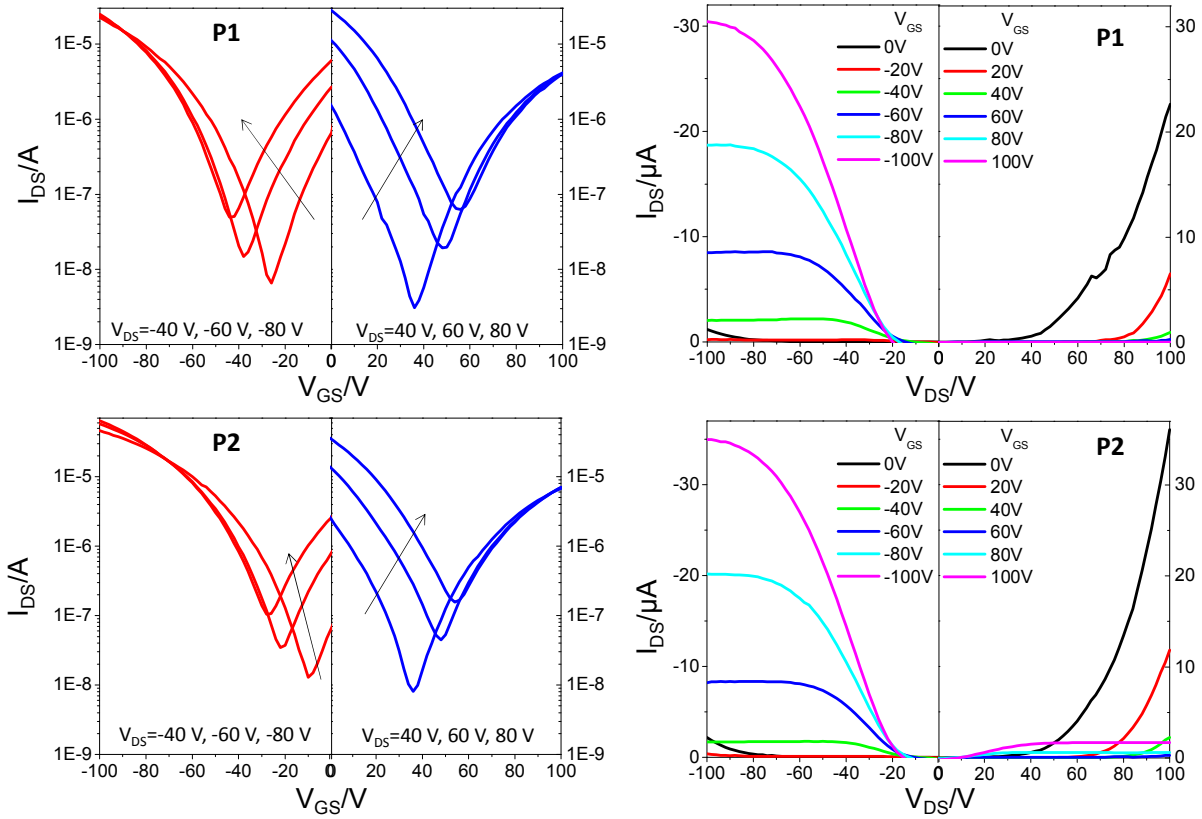

Fig. 4 Transfer (left) and output (right) curves of OTFT devices based on **P1** (annealed at 150 °C) and **P2** (annealed at 200 °C) thin films. Device dimensions: channel length, L = 30 μm; channel width, W = 1000 μm.

than that of their EBI analogous **PEBIBT-24** (0.353 nm).[20] The large π-π distance observed for **P1** and **P2** might be due to the weaker intermolecular interaction of the H-aggregated polymer chains discussed previously.

The thin film morphology is known to influence the charge transport performance greatly. It has been found that a morphology containing well interconnected grains with small grain boundaries is desirable for efficient charge carrier hopping between grains.[10-12] The 100 °C-annealed **P1** film showed well connected grains of ~100-200 nm in its atomic force microscopic (AFM) image, where each grain consists of smaller oval-shaped sub-grains (Fig. 3). Upon increasing the annealing temperature to 150 °C and 200 °C, the sub-grains have become more clearly defined, but the film morphology maintained similar. **P2** films showed similar morphologies to those of **P1** films, but the grains and sub-grains are much larger than those of **P1**. Since the XRD results showed that **P2** films are less crystalline than **P1**, the sizes of the grains and sub-grains seem not correlated to the crystallinity of the thin films.

P1 and **P2** showed a 5 % weight loss temperature ($T_{-5\%}$) at ~380 °C under nitrogen as determined by thermal gravimetric analysis (TGA) (ESI†), which is much higher than that of their EBI counterpart **PEBIBT-24** ($T_{-5\%}$ = ~287 °C).[20] Therefore it appears that the azine (C=N–N=C) linkage in HBI is much more thermally stable than the 1,4-butadiene linkage (C=CH–CH=C) linkage in EBI. No obvious thermal transitions were detected by differential scanning calorimetry (DSC) in the range from -20 °C to 325 °C, indicating the high melting points of these two HBI polymers (ESI).

P1 and **P2** were tested as channel semiconductors in bottom-gate bottom contact OTFT devices using conductive n^{++}-doped silicon wafer with a 300 nm thermally grown SiO_2 layer as a substrate and gold source and drain contacts. The surface of the SiO_2 dielectric layer was treated with dodecyltrichlorosilane before the polymer semiconductor was deposited by spin-coating a polymer solution (5 mg mL^{-1} in $CHCl_3$) in a glove box filled with nitrogen. The devices were annealed at different temperatures and measured in the same glove box. Both polymers showed ambipolar charge transport characteristics (Table 1 and Fig. 4). The best hole/electron mobilities for **P1** are 0.10/0.011 $cm^2V^{-1}s^{-1}$, respectively, which were achieved for a 150 °C-annealed film. For **P2**, the best hole mobility of 0.11 $cm^2V^{-1}s^{-1}$ was obtained for a polymer film annealed at 200 °C, while the highest electron mobility of 0.035 $cm^2V^{-1}s^{-1}$ was achieved for a film annealed at 250 °C. The hole mobilities of **P1** and **P2** are 2-3 times of those of their EBI-based analogous polymers (0.028-0.044 $cm^2V^{-1}s^{-1}$).[20] The improvement in mobility observed for **P1** and **P2** with respect to their EBI analogues is considered to be primarily due to their improved crystallinity, although their π-π distance is larger than the latter. The appearance of electron transport performance of these polymers is most likely originated from the strong electron-accepting capability of the HBI building block that results in low-lying LUMO levels (~-4 eV).

Experimental

Materials and Instrumentation

Reagents and solvents were purchased from commercial sources and used as received without further purification. NMR data were recorded on a Bruker DPX 300 MHz spectrometer and referenced to tetramethylsilane (TMS, 0 ppm). UV-Vis spectra were recorded using a Thermo Scientific Genesys 10 UV instrument. A Digi-Ivy DY2111 potentiostat was used to measure cyclic voltammetry (CV) in 0.1 M tetrabutylammonium hexafluorophosphate in anhydrous acetonitrile at a scan rate of 50 mVs^{-1} under nitrogen protection. An Ag/AgCl reference electrode, a Pt wire counter electrode, and a Pt disk working electrode were used. Ferrocene (Fc) (with a HOMO energy level of -4.8 eV) [36, 37] was used as a reference. Differential scanning calorimetry (DSC) measurements were conducted on a TA Instruments DSC Q2000 at a scan rate of 10 °C min^{-1} under nitrogen protection. Thermal gravimetric analysis (TGA) was conducted on a TA Instruments TGA Q500 at a heating rate of 10 °C min^{-1} under nitrogen protection. An Agilent 1200 series GPC (gel-permeation chromatography) system was used to determine the molecular weight of the polymers using chlorobenzene as an eluent with polystyrene as standards at a column temperature of 50 °C. Reflection X-ray diffraction (XRD) diagrams of polymer thin films spin-coated on dodecyltrichlorosilane-modified SiO_2/Si substrates and annealed at 100, 150, or 200 °C for 15 min in nitrogen were obtained with a Bruker D8 Advance powder diffractometer with Cu Kα radiation (λ = 1.5406 Å). Transmission XRD diagrams of polymer flake samples[42] was performed on a Bruker Smart 600 0 CCD 3-circle D8 diffractometer with a Cu RA (Rigaku) X-ray source (λ = 0.15406 nm). Atomic force microscopic (AFM) images of polymer thin films spin-coated on dodecyltrichlorosilane-modified SiO_2/Si substrates and annealed at 100, 150, or 200 °C for 15 min in nitrogen were obtained using a Dimension 3100 Scanning Probe Microscope.

(3Z,3'Z)-3,3'-(Hydrazine-1,2-diylidene)bis(6-bromoindolin-2-one) (3)

The synthetic scheme for compound **3** is shown in Scheme 1. The procedure is similar to the ones described for the synthesis of other HBI compounds in the references,[29, 30] but with some modifications.

Under argon protection, hydrazine hydrate (98%, 2 mL) was added to a solution of 6-bromoisatin (**1**) (4.265 g, 18.87 mmol) in ethanol (100 mL), a yellow precipitate was formed quickly. The mixture was stirred at 50 °C for 16 h. The precipitate was filtered, washed with ethanol and dried to give (Z)-6-bromo-3-hydrazonoindolin-2-one (**2**) as yellow powder (3.10 g, 68.4%), which is used in the next step without further purification. A mixture of (Z)-6-bromo-3-hydrazonoindolin-2-one (**2**) (3.001 g, 12.5 mmol) and 6-bromoisatin (**1**) (2.825 g, 12.5 mmol) was refluxed in ethanol (150 mL) in the presence of a few drops of acetic acid. After refluxing for 4 h, the reaction mixture was cooled, and filtered. The solid was washed with ethanol, dried to give the reddish brown compound **3** (5.3 g, 94.6%), which was used in the next step without further purification. ^{1}H-NMR (DMSO-d_6, 300 MHz, ppm): δ 11.11 (s, 2H, NH), 7.43 (d, 2H, aromatic), 7.25 (d, 2H, aromatic), 7.09 (s, 2H, aromatic).

(3Z,3'Z)-3,3'-(Hydrazine-1,2-diylidene)bis(6-bromo-1-(2-octyldodecyl)indolin-2-one) (4a)

To a mixture of compound **3** (0.896 g, 2 mmol, 1 equiv.), K_2CO_3 (1.106 g, 8 mmol, 4 equiv.) and anhydrous N,N-dimethylformamide (DMF) (20 mL) in a 50 mL two-necked round bottom flask, 2-octyldodecyl iodide (3.267 g, 8 mmol, 4 equiv.) was added at room temperature,. The reaction mixture was heated with stirring at 50 °C under argon. After 60 h, DMF was evaporated under reduced pressure, and the residue was washed with water, extracted with dichloromethane (DCM), dried over Na_2SO_4, and filtered. The solvent in the filtrate was evaporated under vacuum to give a brown crude product, which was further purified through column chromatography (silica gel, dichloromethane:hexane 1:3) to give the compound **4a** as a brown solid (0.846 g , 41.9%). ^{1}H-NMR ($CDCl_3$, 300 MHz, ppm): δ 9.08 (d, 2H, aromatic, J = 8.7 Hz), 7.16 (dd, 2H, aromatic, J_1 = 8.7 Hz, J_2 =1.8 Hz), 6.90 (d, 2H, aromatic, J = 1.8 Hz), 3.63 (d, 2H, N-CH_2, J = 7.5 Hz), 1.97-1.80 (m, 2H, CH), 1.50-1.10 (m, 64H, CH_2), 0.95-0.75 (m, 12H, CH_3). ^{13}C-NMR (CDCl3, 75 MHz, ppm): 168.19, 146.30, 132.65, 131.16, 126.79, 125.21, 120.49, 111.64, 44.81, 36.21, 32.07, 32.02, 31.62, 30.13, 29.79, 29.77, 29.75, 29.69, 29.50, 29.44, 26.50, 22.85,22.82,14.28,14.27. HRMS (ESI, M + H^+): Found: 979.5336, Cacld.: 979.5291.

(3Z,3'Z)-3,3'-(Hydrazine-1,2-diylidene)bis(6-bromo-1-(2-decyltetradecyl)indolin-2-one) (4b)

4b was synthesized and purified similarly using the procedure described for **4a** from compound **1** (0.896 g, 2 mmol, 1 equiv.) and 2-decyltetradecyl iodide (3.716 g, 8 mmol, 4 equiv.). **4b** was obtained as deep reddish brown solid (0.810 g, 36.1% yield). ^{1}H-NMR ($CDCl_3$, 300 MHz, ppm): δ 9.07 (d, 2H, aromatic, J = 8.7 Hz), 7.17 (dd, 2H, aromatic, J_1 = 8.7 Hz, J_2 =1.8 Hz), 6.90 (d, 2H, aromatic, J = 1.8 Hz), 3.62 (d, 2H, N-CH_2, J = 7.2 Hz), 1.97-1.80 (m, 2H, CH), 1.50-1.10 (m, 80H, CH_2), 0.95-0.75 (m, 12H, CH_3). ^{13}C-NMR (CDCl3, 75 MHz, ppm): 168.26, 146.36, 132.74, 131.16, 126.82, 125.26, 120.53, 111.70, 44.83, 36.22, 32.08, 31.62, 30.14, 29.79, 29.52, 26.50, 22.85, 14.29. HRMS (ESI, M + H^+): Found: 1091.6575, Cacld.:1091.6543.

Polymer P1

To a 25 mL dry Schlenk flask were added compound **4a** (225.6 mg, 0.2236 mmol), 5,5'-bis(trimethylstannyl)bithiophene (110.0 mg, 0.2236 mmol) and tri(*o*-totyl)phosphine (5.4 mg, 8 mol %, 17.6 μmol). After degassing and refilling argon 3 times, tris(dibenzylideneacetone)-dipalladium (4.0 mg, 2 mol %, 4.4 μmol) and dry chlorobenzene (5 ml) were added under an argon atmosphere. The reaction mixture was stirred at 130 °C for 72 h. The reaction mixture was then cooled to room temperature and poured into a stirring methanol (60 ml) and stirred for 2 h. The precipitate was collected by filtration, and subjected to consecutive Soxhlet extraction with acetone, hexane and chloroform. Evaporating the solvent from the chloroform extraction gave **P1** as a deep blue solid (220.0 mg, 97.1%). GPC (with chlorobenzene as an eluent and measured at 50 °C): the number average molecular weight (M_n) = 40,020; the weight average molecular weight (M_w) = 89,209; polydispersity index (PDI) = 2.23. λ_{max} (~10^{-5} M in chloroform): 706 nm.

Polymer P2

P2 was synthesized and purified similarly using the procedure described for **P1** from compound **4b** (257.0 mg, 0.2292 mmol), and 5,5'-bis(trimethylstannyl)bithiophene (112.7 mg, 0.2292 mmol). The resulted crude product was purified by consecutive Soxhlet extraction with acetone, hexane and chloroform. Lower

molecular weight portion was obtained from the hexane extraction (139 mg, 54.0%). The higher molecular weight **P2** was obtained from chloroform extraction as deep-blue films (115 mg, 44.6% yield). GPC (with chlorobenzene as an eluent and measured at 50 °C): M_n = 49,789; M_w = 87,743; PDI = 1.76. λ_{max} (~10^{-5} M in chloroform): 706 nm.

OTFT Fabrication and characterization

A bottom-gate bottom-contact OTFT structure was adopted. A heavily n^{++}-doped Si wafer with a thermally SiO_2 layer (~300 nm) (with a capacitance of ~11.6 nF cm^{-2}) was used as the substrate. The gold source and drain electrode pairs were patterned on the SiO_2/Si substrate by thermal evaporation using a routine lithography procedure. The substrate was washed with acetone and isopropanol, cleaned with O_2 plasma, and then dipped in a dodecyltrichlorosilane (DDTS) solution in toluene (10 mg mL^{-1}) at 60 °C for 20 min to form a DDTS monolayer on the SiO_2 surface. After washing with toluene and drying under a nitrogen flow, a polymer (**P1** or **P2**) solution in chloroform (5 mg mL^{-1}) was spin-coated on the substrate at 3000 rpm for 60 s to form a polymer film (~35 nm), which was annealed at 150 °C or 200 °C on a hotplate for 15 min in a glove box filled with nitrogen. The OTFT devices were characterized in the same glove box using an Agilent B2912A Precision Source/Measure Unit. The charge carrier mobility in the saturated regime, μ_{sat}, is calculated using the equation: $I_{DS} = C_i \mu_{sat} (W/2L) (V_G-V_T)^2$, whereas I_{DS} is the drain current, C_i is the capacitance per unit area of the gate dielectric, W and L are the semiconductor channel width and length, respectively, V_G is the gate voltage, and V_T is the threshold voltage, which is the V_G axis intercept of the linear extrapolation of the $(I_{DS})^{1/2}$ - V_G curve in the saturation regime at I_{DS} = 0. All the devices have a channel length (L) of 30 μm and a channel width (W) of 1000 μm.

Conclusions

We reported the use of a novel electron-accepting building block, (3Z,3'Z)-3,3'-(hydrazine-1,2-diylidene)bis(indolin-2-one) (HBI), for constructing donor-acceptor copolymers with a bithiophene donor. The resulting polymers exhibited ambipolar charge transport performance in OTFTs with hole and electron mobilties up to 0.11 $cm^2V^{-1}s^{-1}$ and 0.035 $cm^2V^{-1}s^{-1}$, respectively. The much improved hole mobility is considered to be due to the higher crystallinity of these HBI-based polymers as compared with their analogous 3,3'-(ethane-1,2-diylidene)bis(indolin-2-one) (EBI)-based polymers. The observed electron transport performance of these polymers is attributed to the strong electron accepting effect of the HBI building block. The HBI-based polymers also exhibited much superior thermal stability. This study shows that HBI is a very promising electron acceptor building block for polymer semiconductors for OTFTs, OPVs, and other organic electronics. It is also demonstrated again that azine is a very useful conjugated backbone linkage for high performance polymer semiconductors, which can be easily synthesized with established chemistries and are thermally stable.

Acknowledgements

The authors thank the Natural Sciences and Engineering Research Council (NSERC) of Canada for the financial support (Discovery Grants #402566-2011) of this work. The authors also thank Dr. Changsheng Wang of Merck Chemicals Ltd. for measuring molecular weights of polymers using GPC.

Notes and references

[a] Department of Chemical Engineering and Waterloo Institute for Nanotechnology (WIN), 200 University Ave W, Waterloo, Ontario, N2L 3G1, Canada; Fax: +1 519-888-4347; Tel: +1 519-888-4567 ext. 31105; Email: yuning.li@uwaterloo.ca.

† Electronic Supplementary Information (ESI) available.

‡ These authors contributed equally.

Electronic Supplementary Information (ESI) available: [details of any supplementary information available should be included here]. See DOI: 10.1039/b000000x/

1. A. C. Arias, J. D. MacKenzie, I. McCulloch, J. Rivnay and A. Salleo, *Chemical Reviews*, 2010, **110**, 3-24.
2. H. Klauk, *Chemical Society Reviews*, 2010, **39**, 2643-2666.
3. A. Facchetti, *Materials Today*, 2013, **16**, 123-132.
4. L. Torsi, M. Magliulo, K. Manoli and G. Palazzo, *Chemical Society Reviews*, 2013, **42**, 8612-8628.
5. H. Sirringhaus, *Advanced Materials*, 2014, **26**, 1319-1335.
6. J. Chen and Y. Cao, *Accounts of Chemical Research*, 2009, **42**, 1709-1718.
7. Y. J. Cheng, S. H. Yang and C. S. Hsu, *Chemical Reviews*, 2009, **109**, 5868-5923.
8. P. L. T. Boudreault, A. Najari and M. Leclerc, *Chemistry of Materials*, 2010, **23**, 456-469.
9. R. S. Kularatne, H. D. Magurudeniya, P. Sista, M. C. Biewer and M. C. Stefan, *Journal of Polymer Science Part A: Polymer Chemistry*, 2013, **51**, 743-768.
10. Y. Li, P. Sonar, L. Murphy and W. Hong, *Energy & Environmental Science*, 2013, **6**, 1684-1710.
11. Y. He, W. Hong and Y. Li, *Journal of Materials Chemistry C*, 2014, **2**, 8651-8661.
12. C. Guo, W. Hong, H. Aziz and Y. Li, *Reviews in Advanced Sciences and Engineering*, 2012, **1**, 200-224.
13. J. Li, Y. Zhao, H. S. Tan, Y. Guo, C.-A. Di, G. Yu, Y. Liu, M. Lin, S. H. Lim, Y. Zhou, H. Su and B. S. Ong, *Sci. Rep.*, 2012, **2**, 754.
14. I. Kang, H. J. Yun, D. S. Chung, S. K. Kwon and Y. H. Kim, *Journal of the American Chemical Society*, 2013, **135**, 14896-14899.
15. G. Kim, S. J. Kang, G. K. Dutta, Y. K. Han, T. J. Shin, Y. Y. Noh and C. Yang, *Journal of the American Chemical Society*, 2014, **136**, 9477-9483.
16. B. Sun, W. Hong, Z. Yan, H. Aziz and Y. Li, *Advanced Materials*, 2014, **26**, 2636-2642.
17. H.-J. Yun, S.-J. Kang, Y. Xu, S. O. Kim, Y.-H. Kim, Y.-Y. Noh and S.-K. Kwon, *Advanced Materials*, 2014, **26**, 7300-7307.
18. X. Guo, A. Facchetti and T. J. Marks, *Chemical Reviews*, 2014, **114**, 8943-9021.
19. A. Pron and M. Leclerc, *Progress in Polymer Science*, 2013, **38**, 1815-1831.
20. S. Chen, B. Sun, C. Guo, W. Hong, Y. Meng and Y. Li, *Chemical Communications*, 2014, **50**, 6509-6512.
21. M. Păstrăvanu, M. Dumitriu and T. Lixandru, *European Polymer Journal*, 1981, **17**, 197-201.

22. C. R. Hauer, G. S. King, E. L. McCool, W. B. Euler, J. D. Ferrara and W. J. Youngs, *Journal Of The American Chemical Society*, 1987, **109**, 5760-5765.
23. Y. Cao and S. Li, *Journal of the Chemical Society, Chemical Communications*, 1988, 937-938.
24. W. B. Euler, *Chemistry Of Materials*, 1990, **2**, 209-213.
25. D. S. Dudis, A. T. Yeates, D. Kost, D. A. Smith and J. Medrano, *Journal Of The American Chemical Society*, 1993, **115**, 8770-8774.
26. W. B. Euler, *Chemistry Of Materials*, 1996, **8**, 554-557.
27. A. Faccinetto, S. Mazzucato, D. Pedron, R. Bozio, S. Destri and W. Porzio, *Chemphyschem*, 2008, **9**, 2028-2034.
28. W. Hong, B. Sun, H. Aziz, W. T. Park, Y. Y. Noh and Y. N. Li, *Chemical Communications*, 2012, **48**, 8413-8415.
29. *US Pat.*, US20120252860 A1, 2012.
30. C. Liang, J. Xia, D. Lei, X. Li, Q. Yao and J. Gao, *European Journal Of Medicinal Chemistry*, 2014, **74**, 742-750.
31. S. Chen, B. Sun, W. Hong, H. Aziz, Y. Meng and Y. Li, *Journal of Materials Chemistry C*, 2014, **2**, 2183-2190.
32. C. Scharsich, R. H. Lohwasser, M. Sommer, U. Asawapirom, U. Scherf, M. Thelakkat, D. Neher and A. Kohler, *J. Polym. Sci. Pt. B-Polym. Phys.*, 2012, **50**, 442-453.
33. J. Lee, A. R. Han, J. Kim, Y. Kim, J. H. Oh and C. Yang, *Journal of the American Chemical Society*, 2012, **134**, 20713-20721.
34. J. Shin, H. A. Um, D. H. Lee, T. W. Lee, M. J. Cho and D. H. Choi, *Polymer Chemistry*, 2013, **4**, 5688-5695.
35. F. C. Spano and C. Silva, *Annual Review Of Physical Chemistry*, 2014, **65**, 477-500.
36. J. Pommerehne, H. Vestweber, W. Guss, R. F. Mahrt, H. Bässler, M. Porsch and J. Daub, *Advanced Materials*, 1995, **7**, 551-554.
37. B. W. D'Andrade, S. Datta, S. R. Forrest, P. Djurovich, E. Polikarpov and M. E. Thompson, *Organic Electronics*, 2005, **6**, 11-20.
38. E. Conwell, in *Primary Photoexcitations in Conjugated Polymers: Molecular Excitons versus Semiconductor Band Model* ed. N. S. Sariciftci, World Scientific Singapore, 1997.
39. Y. Zhu, R. D. Champion and S. A. Jenekhe, *Macromolecules*, 2006, **39**, 8712-8719.
40. T.-A. Chen, X. Wu and R. D. Rieke, *Journal of the American Chemical Society*, 1995, **117**, 233-244.
41. H. Sirringhaus, P. J. Brown, R. H. Friend, M. M. Nielsen, K. Bechgaard, B. M. W. Langeveld-Voss, A. J. H. Spiering, R. A. J. Janssen, E. W. Meijer, P. Herwig and D. M. de Leeuw, *Nature*, 1999, **401**, 685-688.
42. H. Pan, Y. Li, Y. Wu, P. Liu, B. S. Ong, S. Zhu and G. Xu, *Journal of the American Chemical Society*, 2007, **129**, 4112-4113.

Graphical abstract

(3Z,3'Z)-3,3'-(Hydrazine-1,2-diylidene)bis(indolin-2-one) (HBI) is found to be a promising novel building block for polymer semiconductors.